Activation cross-sections for short-lived reaction products on hafnium isotopes induced by 1 – 20 MeV neutrons

Valentina Semkova[1*], *Anguel* Demerdjiev[1], *André* Moens[2], *Naohiko* Otuka[3], *Arjan* Plompen[2], and *Dimitar* Tonev[1]

[1]Institute for Nuclear Research and Nuclear Energy, Bulgarian Academy of Sciences, 1784 Sofia, Bulgaria
[2] European Commission, Joint Research Centre, 2440 Geel, Belgium
[3]Nuclear Data Section, International Atomic Energy Agency, 1400 Wien, Austria

Abstract. Results of new activation cross-section measurements for production of ^{178m1}Hf ($T_{1/2}$ = 4.0 s) and ^{179m1}Hf ($T_{1/2}$ = 18.67 s) are presented for the following reactions: ^{178}Hf(n,n´)^{178m1}Hf, ^{179}Hf(n,2n)^{178m1}Hf, ^{180}Hf(n,3n)^{178m1}Hf, ^{179}Hf(n,n´)^{179m1}Hf, and ^{180}Hf(n,2n)^{179m1}Hf. The irradiations were carried out at the 7-MV Van de Graaff accelerator at EC-JRC, Geel. Neutrons in the 1-3 MeV energy range were produced via the ^{3}H(p,n)^{3}He reaction. Deuteron beam and a deuterium gas target were used to produce 5 and 6 MeV neutrons. For the production of quasi-monoenergetic neutrons between 16 and 19.5 MeV the ^{3}H(d,n)^{4}He reactions was employed. Both samples with natural composition and isotopic enrichment were employed to differentiate reactions leading to the same product. An automated pneumatic system was used for the sample irradiation, transport and radioactivity measurements. The radioactivity of the samples was determined by standard gamma-spectrometry using HPGe detector. The results obtained in the present work are compared with the data from other authors and TENDL-2017 evaluation.

1 Introduction

Neutron-induced reaction cross-sections on hafnium isotopes are important for research and nuclear applications. Hafnium is considered as a constituent of the control elements and structural materials of nuclear reactors due to its high absorption cross-section for slow neutrons, good mechanical properties and extremely high resistance to corrosion. Hafnium is an alloying element of low activation materials. Many of the neutron-induced reactions on hafnium isotopes populate metastable states. Experimental cross-sections provide a database for investigation of the sensitivity of nuclear models to level properties and decay schemes. Activation cross-section data for short-lived reaction products on hafnium isotopes are scarce. The results obtained in the present work are compared with the data from other authors from the EXFOR database [1] and the TENDL-2017 evaluation [2].

2 Experimental procedure

The neutron-induced reaction cross sections obtained in the present work have been measured by the activation technique.

The irradiations were carried out at the 7 MV Van de Graaff accelerator at EC-JRC Geel. Neutrons in the energy range 1.3–3.0 MeV were produced by a proton beam incident on a solid-state Ti-T target via the ^{3}H(p, n)^{3}He reaction (Q = −0.764 MeV). The energies of the protons were between 2.2 and 3.9 MeV. A deuterium gas target was used for production of neutrons with energies of 5 and 6 MeV via the ^{2}H(d,n)^{3}He reaction (Q = 3.269 MeV) at incident deuteron energies of 2 and 3 MeV, respectively. The target cell was 4 cm in length and 4 cm in diameter with a 5 μm molybdenum entrance foil. Quasi-monoenergetic neutrons with energies between 16.5 and 19.5 MeV were produced via the ^{3}H(d,n)^{4}He reaction (Q = 17.59 MeV) at incident deuteron energies of 1, 2 and 3 MeV. The time profile of the neutron flux during the irradiations was monitored by a BF3 long counter operating in a multichannel scaling acquisition mode. The samples were irradiated at 0 degree relative to the incident ion beam at 16 mm distance from the back of the target. A pneumatic transport system was used for the sample transport between the irradiation and activity measurement positions. The sample transport was controlled by the DAQ2000 system developed at JRC-Geel. A multichannel scaler is used to register the neutron-flux time-profile, the time for the sample transport between irradiation and measurement positions as well as the counting period with a resolution of 0.1 s. Simultaneously the gamma-ray spectra from the HPGe detector were recorded. The time for the sample transport was 3.5(1) s. Irradiation times of 120 s and measurement time of 30 s were applied in case of ^{179m1}Hf production cross section measurements. Cycles of 30 s sample irradiations and 6 s activity measurements were carried out in the measurements of the reactions leading to ^{178m1}Hf in order to enhance the counting statistics. A single irradiation of 120 s and activity measurement of

* Corresponding author: vsemkova@inrne.bas.bg

30 s were performed for the ^{179m1}Hf production cross section measurements to minimise the interference between the 214.335 keV and 213.434 keV gamma-lines from the ^{179m1}Hf and ^{178m1}Hf decays. The contribution of the ^{178m1}Hf decay to the 214 keV gamma line intensity was considered as negligible since there were no other gamma-lines from the ^{178m1}Hf decay in the gamma-ray spectra under those irradiation and measurement conditions.

Hafnium consists of six isotopes. Both isotopically enriched and samples with natural isotopic composition were used due to interference between reactions on different isotopes leading to the same reaction product. The isotopic composition of the sample materials employed in the present work is given in Table 1.

Table 1. Isotopic abundance (%) of the hafnium sample material employed in the present work.

	^{nat}Hf	**$^{177}HfO_2$**	**$^{178}HfO_2$**	**$^{179}HfO_2$**
^{174}Hf	0.16(1)	< 0.05	< 0.05	< 0.05
^{176}Hf	5.26(7)	1.0	0.8	0.2
^{177}Hf	18.60(9)	85.4	1.9	1.3
^{178}Hf	27.28(7)	11.3	92.4	4.1
^{179}Hf	13.62(2)	0.9	3.3	72.1
^{180}Hf	35.08(16)	1.4	1.6	22.3

The isotopically enriched samples were prepared by canning about 100 mg of HfO_2 powder in plexiglass containers with 10 mm inner diameter. Metallic disks of 10 mm diameter and 0.1 mm thickness were prepared from natural material of 97% hafnium and 3% zirconium. High purity metallic aluminium, niobium, iron, indium, and nickel foils of 10 mm diameter were used to determine the neutron flux and flux density distribution at different incident neutron energies.

The cross-sections for the studied reactions were determined relative to the ^{27}Al(n,α)^{24}Na reaction cross section above 16 MeV incident neutron energy. In the energy range below 6 MeV the ^{115}In(n,n´)^{115m}In reaction was used for the neutron flux determination. Data for both the ^{27}Al(n,α)^{24}Na and ^{115}In(n,n´)^{115m}In reaction cross sections were taken from the International Reactor Dosimetry and Fusion File (IRDFF-II) [3].

The mean energy and standard spread of the primary neutrons for the target-sample irradiation geometry were calculated by the NeuSDesc software [4] based on the reaction data and the stopping powers.

The neutron spectra from Ti-T target at 2 and 3 MeV incident deuteron energy consist of primary neutrons from the ^{3}H(d,n)^{4}He reaction and a background of low energy neutron distribution due to scattering and secondary reactions with the target environment. The complexity and intensity of the low-energy neutron distributions depend on incident beam energy, emission angle and history of the target. The neutron flux energy distribution for each irradiation was determined by the method of spectral indexing [5] based on the TOF measurements of the laboratory neutron spectra and well-characterized standard activation cross-sections with different thresholds. The parameters of the few-group spectral representations were adjusted by the method of generalized least squares using the known response characteristics of the spectral-index reactions. The following reactions were used in the unfolding procedure: ^{27}Al(n,α)^{24}Na, ^{115}In(n,n´)^{115m}In, ^{58}Ni(n,p)^{58}Co, ^{56}Fe(n,p)^{56}Mn, ^{27}Al(n,p)^{27}Mg, ^{93}Nb(n,2n)^{92m}Nb. Evaluated cross sections from the International Reactor Dosimetry and Fusion File (IRDFF-II) [3] for all reactions were used in the analysis.

The flux density distribution at each incident neutron energy was determined by a separate irradiation of a stack of monitor foils. The count rates from the BF3 long counter were used for the normalization of the neutron flux during the short irradiations.

The radioactivity of the reaction products was determined by gamma-ray spectrometry. Two HPGe detectors were used for the radioactivity measurement. One, attached to the pneumatic transport system, for the measurement of the short-lived reaction products and another for the measurements of the monitor reaction products. The decay data for ^{178m1}Hf [6] and ^{179m1}Hf [7] are given in Table 2.

Table 2. The investigated reactions, the Q-value of the reaction and the decay data of the reaction products.

Nuclear reaction	Q-value (keV)	$T_{1/2}$ (s)	E_γ (keV)	I_g (%)
^{178}Hf(n,n´)^{178m1}Hf	-1147	4.0	325.6	94.1
^{179}Hf(n,2n)^{178m1}Hf	-7246	4.0	325.6	94.1
^{180}Hf(n,3n)^{178m1}Hf	-14634	4.0	325.6	94.1
^{179}Hf(n,n´)^{179m1}Hf	- 375	18.67	214.3	95.3
^{180}Hf(n,2n)^{179m1}Hf	-7763	18.67	214.3	95.3

The detector calibration procedure involved several steps. A set of ^{241}Am, ^{109}Cd, ^{57}Co, ^{139}Ce, ^{51}Cr, ^{137}Cs, ^{54}Mn, ^{65}Zn, ^{22}Na and ^{60}Co point standard sources were used to measure the peak and total detector efficiencies $\epsilon_i(E_i, r_i, z_i)$ at reference positions $P(r_i.z_i)$. The detector efficiencies were parametrized by regression analysis with least square fitting of the measured values using polynomial logarithmic function $\ln\epsilon = \sum_{k=1}^{n} p_k(\ln E)^{k-1}$. Correction for coincidence summing effects was applied in the ^{178m1}Hf activity analysis, while for the ^{179m1}Hf analysis the correction factor is negligible.

The measured production rate in the sample is determined by:

$$PR = \frac{\lambda Y}{b\epsilon} \frac{\prod_k c_{ik}}{[1-exp(-\lambda t_{irr})]exp(-\lambda t_w)[1-exp(-\lambda t_{mes})]}$$

where λ is decay constant; Y is the number of measured gamma-ray counts; b is the gamma-ray emission probability; ϵ is the detector full-energy-peak efficiency; t_{irr} is the time of irradiation; t_w is the time from the end of irradiation to the beginning of gamma-ray counting; t_{mes} is the gamma-ray counting time; c_{ik} are correction factors applied. The corrections were applied for the neutron beam intensity fluctuation during the irradiation and gamma-ray self-absorption.

There are more than two reactions contributing to the production of ^{178m1}Hf or ^{179m1}Hf in a hafnium sample with natural isotopic composition, including (n,γ) reaction induced by background neutrons. The cross sections for two (respectively more) interfering reactions were deduced by irradiating samples having different composition. The reaction rates PR_1 and PR_2 due to reactions 1 and 2 contributing to production rates PR_x and PR_y in the sample x and sample y were deduced by the following equations:

$$PR_1 = \frac{N_{y2}PR_x - N_{x2}PR_y}{N_{x1}N_{y2} - N_{x2}N_{y1}}$$
$$PR_2 = \frac{N_{x1}PR_{xy} - N_{y1}PR_x}{N_{x1}N_{y2} - N_{x2}N_{y1}}$$

were N_{x1}, N_{x2}, N_{y1} and N_{y2} are the number of target nuclei for reaction 1 in sample x, reaction 2 in sample x, reaction 1 in sample y, and reaction 2 in sample y. The obtained reaction rates were corrected for the background neutrons and divided by the neutron flux to determine the reaction cross sections.

3 Results and discussion

Results from the present measurements for the reactions leading to production of ^{178m1}Hf are shown in Figure 1 and the reactions leading to production of ^{179m1}Hf are shown in Figure 2. The data from this work are compared with the experimental data from the EXFOR database and the TENDL-2017 evaluation.

3.1 ^{178}Hf(n,n´)^{178m1}Hf, ^{179}Hf(n,2n)^{178m1}Hf, and ^{180}Hf(n,3n)^{178m1}Hf reaction cross sections

Isotopically enriched $^{178}HfO_2$ and $^{179}HfO_2$ samples and sample with natural isotopic composition were used to study the ^{178}Hf(n,n´)^{178m1}Hf, ^{179}Hf(n,2n)^{178m1}Hf and ^{180}Hf(n,3n)^{178m1}Hf reaction cross sections (Fig. 1). Measurements with enriched $^{177}HfO_2$ sample were performed as well in order to take into account the contribution of the ^{178m1}Hf activity from (n,γ) reaction induced by background neutrons on ^{177}Hf.

The 1147.388 keV isomeric state decays by 100% isomeric transition. Five gamma-lines are emitted in a cascade. The 325.557 keV gamma-line was used in the present measurements.

Our results agree within the standard uncertainties with TENDL-2017 evaluation for the ^{179}Hf(n,2n)^{178m1}Hf and the ^{180}Hf(n,3n)^{178m1}Hf reaction cross sections.

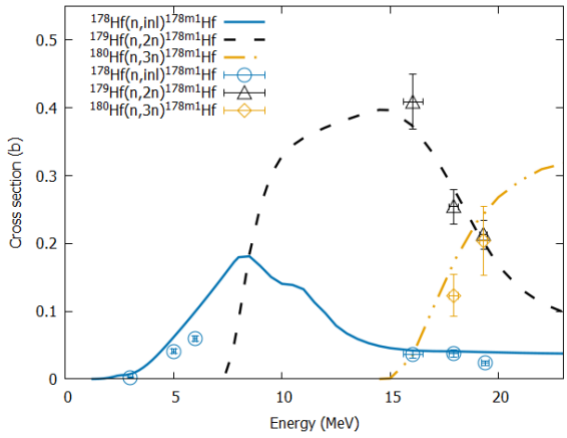

Fig. 1. Comparison between the experimental data from this work (points) and TENDL-2017 evaluation (lines) for the ^{178}Hf(n,n´)^{178m1}Hf, ^{179}Hf(n,2n)^{178m1}Hf and ^{180}Hf(n,3n)^{178m1}Hf reaction cross sections.

There is only one Entry for the ^{179}Hf(n,2n)^{178m1}Hf cross section available in EXFOR database. The result of Prasad *at al.* from1966 [8] (EXFOR subentry 30015.006) of 880 mb at 14.8 keV is higher than our data.

3.2 ^{178}Hf(n,γ)^{179m1}Hf, ^{179}Hf(n,n´)^{179m1}Hf and ^{180}Hf(n,2n)^{179m1}Hf reaction cross sections

Isotopically enriched $^{178}HfO_2$ and $^{179}HfO_2$ samples as well as sample with natural isotopic composition were used to study ^{178}Hf(n,γ)^{179m1}Hf, ^{179}Hf(n,n´)^{179m1}Hf, and ^{180}Hf(n,2n)^{179m1}Hf reaction cross sections (Fig. 2). The ^{115}In(n,γ)^{116m1}In and ^{115}In(n,n´)^{115m}In reaction rates induced by 1.3–3.0 MeV neutrons were consistent within 10%. The ^{178}Hf(n,γ)^{179m1}Hf reaction cross section was determined relative to ^{115}In(n,γ)^{116m1}In IRDFF-II evaluated reaction cross section [3].

Our results for the ^{179}Hf(n,n´)^{179m1}Hf reaction cross section are in agreement with the data of Shimizu *et al.* from 2004 [9] (EXFOR subentry 22838.012) and TENDL-2017 evaluation at low incident neutron energies, but higher than the TENDL-2017 evaluation above 16 MeV.

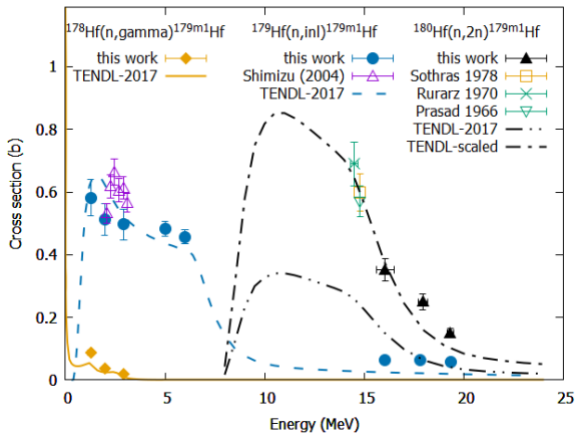

Fig. 2. Comparison between experimental data from this work, TENDL-2017 evaluation, and the data from other authors for the ^{179}Hf(n,n´)^{179m1}Hf and ^{180}Hf(n,2n)^{179m1}Hf reactions cross sections.

Our results for the ^{180}Hf(n,2n)^{179m1}Hf reaction cross section can be considered as consistent with the data of Prasad *at al*. from1966 [8] (EXFOR subentry 30015.007) , Rurarz *et al*. from 1970 [10] (EXFOR subentry 30154.008) and Sothras from 1977 [11] (EXFOR subentry 10835.022) around 14 MeV based on a scaled values of the TENDL-2017 evaluation.

The new results for the ^{178}Hf(n,γ)^{179m1}Hf reaction cross section are about 50% higher than TENDL-2017 evaluation. There are only two Maxwellian average cross section datasets for the ^{178}Hf(n,γ)^{179m1}Hf reaction available in the EXFOR database.

4 Summary and conclusions

Cross sections for the ^{178}Hf(n,n´)^{178m1}Hf, ^{179}Hf(n,2n)^{178m1}Hf, ^{180}Hf(n,3n)^{178m1}Hf, ^{178}Hf(n,γ)^{179m1}Hf, ^{179}Hf(n,n´)^{179m1}Hf, and ^{180}Hf(n,2n)^{179m1}Hf have been studied by activation technique in the energy range from 1 to 20 MeV. In the energy range from 1 to 6 MeV the cross sections were determined relative to the ^{115}In(n,n´)^{115m}In reaction cross section. Above 16 MeV the ^{27}Al(n,α)^{24}Na standard cross section was used for normalization. Both samples with natural composition and isotopic enrichment were employed to differentiate reactions leading to the same product. The new experimental data improve the knowledge of the excitation functions of the investigated reactions and three of the studied reactions were measured for the first time

The authors are grateful to the EC-JRC Geel Van de Graaff Laboratory personnel for providing us with the best possible experimental conditions. V.S. is grateful to the EC-JRC for support to carry out research at EC-JRC Geel. This research has been supported by the National Roadmap for Research Infrastructure 2020-2027 for the National Cyclotron Centre funded by the Bulgarian Ministry of Education and Science.

References

1. N. Otuka, E. Dupont, V. Semkova, B. Pritychenko, A.I. Blokhin, M. Aikawa, S. Babykina, M. Bossant, G. Chen, S. Dunaeva, R.A. Forrest, T. Fukahori, N. Furutachi, S. Ganesan, Z. Ge, O.O. Gritzay, M. Herman, S. Hlavač, K. Katö, B. Lalremruata, Y.O. Lee, A. Makinaga, K. Matsumoto, M. Mikhaylyukova, G. Pikulina, V.G. Pronyaev, A. Saxena, O. Schwerer, S.P. Simakov, N. Soppera, R. Suzuki, S. Takács, X. Tao, S. Taova, F. Tárkányi, V.V. Varlamov, J. Wang, S.C. Yang, V. Zerkin, Y. Zhuang, Nucl. Data Sheets 1**20**, 272 (2014)
2. A.J. Koning and D. Rochman, Nucl. Data Sheets **113**, 2841 (2012)
3. A. Trkov, P.J. Griffin, S.P. Simakov, L.R. Greenwood, K.I. Zolotarev, R. Capote, D.L. Aldama, V. Chechev, C. Destouches, A.C. Kahler, C. Konno, M. Koštál, M. Majerle, E. Malambu, M. Ohta, V.G. Pronyaev, V. Radulovič, S. Sato, M. Schulc, E. Šimečková, I. Vavtar, J. Wagemans, M. White, H. Yashima, Nucl. Data Sheets **163**, 1 (2020)
4. E. Birgersson and G. Lovestam, EUR 23794 (2009)
5. D.L. Smith, A.J.M. Plompen, V. Semkova, NEA-WPEC-19, p. 155 (2005)
6. E. Achterberg, O. A. Capurro, G. V. Marti, Nucl. Data Sheets **110**, 1473 (2009)
7. Coral M. Baglin, Nucl. Data Sheets **110**, 265 (2009)
8. R. Prasad, D.C. Sarkar, C.S.Khurana. Nucl. Phys. **88**, 349 (1966)
9. T. Shimizu, H. Sakane , M. Shibata, K. Kawade, T. Nishitani, Ann. Nucl. Energy **31**, 1883 (2004)
10. E. Rurarz, Z. Haratym, M. Pietrzykowski and A. Sulik, Acta Phys. Polon. **B1**, 415 (1970)
11. S. Sothras, PhD thesis submitted to Southern Methodist University (1977)